Hydrol. Earth Syst. Sci. Discuss., 10, 3795–3842, 2013
www.hydrol-earth-syst-sci-discuss.net/10/3795/2013/
doi:10.5194/hessd-10-3795-2013

Hydrology and Earth System Sciences
Open Access
Discussions

Investigating the spatio-temporal variability in groundwater and surface water interactions: a multi-technical approach

N. P. Unland[1,2], I. Cartwright[1,2], M. S. Andersen[2,3], G. C. Rau[2,3], J. Reed[1], B. S. Gilfedder[1,2], A. P. Atkinson[1,2], and H. Hofmann[1,2]

[1]School of Geosciences, Monash University, Clayton, Vic. 3800, Australia
[2]National Centre for Groundwater Research and Training, GPO box 2100, Flinders University, Adelaide, SA 5001, Australia
[3]Connected Waters Initiative Research Centre (CWI), School of Civil and Environmental Engineering, University of New South Wales, Sydney NSW 2093, Australia

Received: 19 February 2013 – Accepted: 9 March 2013 – Published: 22 March 2013

Correspondence to: N. P. Unland (nicolaas.unland@monash.edu)

Published by Copernicus Publications on behalf of the European Geosciences Union.

Abstract

The interaction between groundwater and surface water along the Tambo and Nicholson Rivers, southeast Australia, was investigated using ^{222}Rn, Cl, differential flow gauging, head gradients, electrical conductivity (EC) and temperature profiling. Head gradients, temperature profiles, Cl concentrations and ^{222}Rn activities all indicate higher groundwater fluxes to the Tambo River in areas of increased topographic variation where the potential to form large groundwater–surface water gradients is greater. Groundwater discharge to the Tambo River calculated by Cl mass balance was significantly lower (1.48×10^4 to 1.41×10^3 m^3 day^{-1}) than discharge estimated by ^{222}Rn mass balance (5.35×10^5 to 9.56×10^3 m^3 day^{-1}) and differential flow gauging (5.41×10^5 to 6.30×10^3 m^3 day^{-1}). While groundwater sampling from the bank of the Tambo River was intended to account for the variability in groundwater chemistry associated with river-bank interaction, the spatial variability under which these interactions occurs remained unaccounted for, limiting the use of Cl as an effective tracer. Groundwater discharge to both the Tambo and Nicholson Rivers was the highest under high flow conditions in the days to weeks following significant rainfall, indicating that the rivers are well connected to a groundwater system that is responsive to rainfall. Groundwater constituted the lowest proportion of river discharge during times of increased rainfall that followed dry periods, while groundwater constituted the highest proportion of river discharge under baseflow conditions (21.4 % of the Tambo in April 2010 and 18.9 % of the Nicholson in September 2010).

1 Introduction

Constraining the interaction between groundwater and rivers is important for calculating water balances and sustainable levels of water extraction (Tsur and Graham-Tomasi, 1991), maintaining healthy river ecology (Boulton, 1993; Krause et al., 2007; Luc, 2004), understanding biogeochemical reactions at the groundwater–surface water interface (Peyrard et al., 2011; Sophocleous, 2002; Woessner, 2000) and determining the source and fluxes of nutrients and solutes carried by rivers. In order to estimate groundwater discharge to rivers and to define gaining and losing reaches, a number of physical, chemical and numerical methods have been developed (Kalbus et al., 2006).

Differential flow gauging uses the difference in river discharge at two points along a reach in order to calculate net gains or losses along that stretch (Cey et al., 1998; Harte and Kiah, 2009; McCallum et al., 2012; Ruehl et al., 2006). Discharge is usually measured under baseflow conditions where runoff is negligible, allowing the net groundwater discharge or recharge to be calculated once evaporative losses are accounted for. While gauging stations are usually spaced far apart and often overlook variations at smaller spatial scales, long time series of measurements are commonly available, allowing for analysis of temporal trends and comparative analysis with other methods (McCallum et al., 2013).

As groundwater temperature is commonly higher than that of surface water in winter and lower in summer (Anibas et al., 2009), measurement of temperature in rivers and streambeds can be used to identify gaining and losing reaches (Anderson, 2005; Andersen and Acworth, 2009; Anibas et al., 2011; Rau et al., 2010; Silliman and Booth, 1993). While quantification of water fluxes using temperature requires detailed subsurface temperature measurements over time, temperature mapping of rivers is a simple and effective method of identifying gaining and loosing reaches (Becker et al., 2004). Similarly, if groundwater has a significantly different EC to surface water, changes in river EC can be used to quantify the influx of groundwater (Cartwright et al., 2011; Cey et al., 1998; McCallum et al., 2012). The advantage of along-river temperature/EC surveying is that it allows data to be obtained at a higher spatial resolution than flow gauging or discrete sampling for chemical analysis.

Geochemical tracers including major ions, stable isotopes and radiogenic isotopes have been used to estimate groundwater fluxes in gaining rivers (Cartwright et al., 2010, 2011; Cook et al., 2003, 2006, 2012; Durand et al., 1993; Genereux et al., 1993; Genereux and Hemond, 1990; Lamontagne et al., 2005, 2008; Lamontagne and Cook,

HESSD
10, 3795–3842, 2013

N. P. Unland et al.

2007; Mullinger et al., 2007, 2009; Négrel et al., 2003; Rhode, 1981; Ribolzi et al., 2000; Stellato et al., 2008). The strengths and weaknesses of each of these tracers depends on a variety of factors including the difference between the concentration of the tracer in groundwater compared to surface water, its spatial variability, the accurate characterisation of its sources and sinks and the potential for it to change by processes such as evaporation, precipitation, radioactive decay, degassing, or biogeochemical reactions.

^{222}Rn is produced by the alpha decay of ^{226}Ra in the ^{238}U to ^{206}Pb decay series. Since the concentration of ^{226}Ra in aquifer minerals is several orders of magnitude higher than the concentrations of dissolved ^{226}Ra in surface water, ^{222}Rn activities in groundwater are usually 2–3 orders of magnitude higher than in surface water, making it an effective tracer of groundwater discharge (e.g. Cook et al., 2006, 2012). The use of ^{222}Rn as a groundwater tracer has increased over the last two decades as methods for its measurement in the field have improved (Cartwright et al., 2011; Cook et al., 2003; Ellins et al., 1990; Genereux and Hemond, 1990; Gilfedder et al., 2012; Hofmann et al., 2011; Mullinger et al., 2007, 2009; Santos and Eyre, 2011). Furthermore, as ^{222}Rn has a short half life (3.82 days) and degasses to the atmosphere, river water will only contain elevated activities of ^{222}Rn close to zones of groundwater discharge.

The effectiveness of ^{222}Rn as a groundwater tracer can be limited by poorly-defined groundwater end members and low surface water concentrations which can lead to high analytical uncertainties. The uncertainties associated with the groundwater end members can be reduced by combining groundwater measurements with laboratory experiments in which the ^{226}Ra in sediments is allowed to achieve secular equilibrium with ^{226}Ra/^{222}Rn free water, thus giving the approximate ^{222}Rn activity of water entering the stream (Burnett et al., 2008; Cook et al., 2006; Martens et al., 1980; Peterson et al., 2010). Furthermore, recent work has focussed on better quantifying processes such as hyporheic exchange and gas transfer, making the use of ^{222}Rn more reliable (Cook et al., 2006; Lamontagne and Cook, 2007; Mullinger et al., 2007).

HESSD
10, 3795–3842, 2013
Groundwater – surface water interactions
N. P. Unland et al.

This study uses major ion chemistry, differential flow gauging, and ^{222}Rn activities to calculate groundwater fluxes to the Nicholson and Tambo Rivers and assess how groundwater fluxes vary in response to seasonal changes in rainfall and river discharge. These techniques are combined with EC and temperature mapping to evaluate the detailed spatial variability's of groundwater discharge. By combining a range of techniques, the applicability of each can be assessed through comparative analysis. Furthermore, by conducting the study on two rivers in the same catchment, controls on the gaining and loosing behaviour of neighbouring rivers can be investigated. Taking a multi-technical approach to such investigations is uncommon and can provide additional and more robust information on groundwater–surface water studies (Cox et al., 2007).

1.1 Study area

The Tambo and Nicholson Rivers occur within the Tambo River Basin (Fig. 1), which has a total surface area of ~4200 km^2. These are perennial rivers that drain southwards from the Eastern Victorian Uplands across the Gippsland Basin to Lake King (a saline coastal lake connected to the Tasman Sea). The lake system is affected by tidal forcing which propagates into the lower sections of both the Nicholson and the Tambo rivers, forming estuarine sections that extend ~15 km upstream from the lake during low flow conditions. The river sections do not contain significant tributaries and minor creeks were not flowing during the sampling campaigns.

Average annual precipitation in the catchment is ~705 mm, increasing from 655 mm in the upper catchment to 777 mm in the mid-lower reaches. Precipitation is relatively even year round, with slightly higher than average monthly rainfall during October to December (Bureau of Meteorology, 2012). Annual evapotranspiration rates decrease from 600–700 mm in the upper catchment to 500–600 mm in the lower catchment. During the study period, evaporation ranged from 6.7×10^{-3} m day^{-1} in April 2011 to 3.6×10^{-3} m day^{-1} during August 2011 (Bureau of Meteorology, 2012). Approximately

HESSD
10, 3795–3842, 2013
Groundwater – surface water interactions
N. P. Unland et al.

80 % of the catchment area is covered by forest and woodland, with the remainder dominated by cattle grazing on river floodplains (Department of Agriculture, Fisheries and Forestry, 2006).

The geology of the northern region of the Tambo River Basin is dominated by Ordovician gneisses and schists and Silurian-Devonian granites that form a fractured rock aquifer (Chaplin, 1995; Jolly, 1997). The southern section of the basin is dominated by Tertiary sands and gravels (of the Haunted Hills Gravels and Baxter Sandstone) and Quaternary sands, silts, and calcareous sands of the Shepparton Formation (Fig. 1). Various dune/beach deposits, alluvium and colluvium are locally present with the Tertiary and Quaternary units. While very little is known about the bedrock aquifers in the area, the Tambo and Nicholson rivers flow through an Upper Tertiary aquifer of sands, gravels and clays in the lower catchment and has groundwater with a total dissolved solids (TDS) content of 500–1000 $mg\,L^{-1}$. This overlies Middle and Lower Tertiary aquifers dominated by calcareous sands, gravels, coal and basalt that contain groundwater with a TDS of 1000–3000 $mg\,L^{-1}$.

2 Methods

2.1 River surveys and flow gauging

River discharge is measured at Sarsfield on the Nicholson River and at Ramrod Creek and Battens Landing at on the Tambo River (Victorian Water Resource Warehouse, 2012). In the absence of runoff, significant tributaries or changes in the storage of a river channel, the groundwater flux to a river can be calculated from

$$Q_f = Q_d + E - Q_u - P \tag{1}$$

(Lerner et al., 1990), where Q_f is the groundwater flux, Q_d is the river discharge at the downstream site, Q_u is the river discharge at a upstream site, E is direct evaporation and P is direct precipitation.

HESSD
10, 3795–3842, 2013
Groundwater – surface water interactions
N. P. Unland et al.

The groundwater flux to the Tambo River was calculated using Eq. (1) and the difference in river discharge between Battens Landing and Ramrod creek gauging stations. The difference in the timing of discharge events between the two stations was accounted for by time shifting the discharge of data of the Ramrod Creek gauging station so that discharge events matched (McCallum et al., 2013). When discharge events did not occur during sampling periods (i.e. baseflow conditions), the Ramrod Creek data was time shifted using the distance between the stations and river velocity to calculate the lag time. Q_f estimates were based on the discharge data for a period of ~ 48 h leading up to and including sampling. Direct evaporation and rainfall were calculated using the surface area of the river and data from the Bairnsdale Airport weather station (Bureau of Meteorology, 2012).

Run-of-the-river continuous surface water EC/temperature surveys were conducted during the February 2010 and March 2012 sampling campaigns using a Schlumberger CTD-Diver and an Aqua TROLL 200 logger. Elevation and location during the surveys were recorded using a Trimble DGPS. The elevation of bores and the Tambo River adjoining the bores was also measured using a Trimble DGPS in February 2011, with the elevation in subsequent campaigns interpolated from river height data taken at the Battens Landing and Ramrod Creek gauging stations. Groundwater levels in bores were measured using an electronic water tape during the sampling campaigns. Groundwater-surface water gradients were calculated at Locations 1 and 2 using the measured groundwater elevations of the bore closest to the river and river elevations interpolated from gauging data and DGPS measurements. Gradients were only calculated at Location 3 during February 2011 as upstream gauging does not account for the tidal nature of the location and could not be used to interpolate river height in subsequent campaigns. River depth and width in upstream reaches was measured in the field using a tape measure, while wider downstream reaches were estimated using Google Earth.

HESSD
10, 3795–3842, 2013

2.2 Sampling

Investigations were carried out between the upper catchment and the coastal plain of the Tambo and Nicholson Rivers (Fig. 1). Six sampling campaigns were conducted on a ∼40 km section of the Tambo River and a ∼21 km section of the Nicholson River between April 2010 and March 2012. Sample locations are designated by distance upstream from Lake King. There are 12 sampling locations on the Tambo River and 5 on the Nicholson River. Sampling in April 2010 was conducted at near base flow conditions, while sampling in September 2010 took place during the recession of a minor discharge event (Fig. 2). Sampling in February 2011 occurred during a discharge event while the April 2011 campaign was conducted during low flow conditions after a minor discharge event. Sampling campaigns conducted during August 2011 and March 2012 both took place during the recession of major flood events. Water table measurements and groundwater sampling were conducted in conjunction with river sampling but excluded April 2010 and September 2010 campaigns, as bores were still under construction at these times. Groundwater was sampled at three locations along the Tambo River. Three bores were sampled at Location 1 (28.5 km), two at Location 2 (20.2 km) and 1 at Location 3 (13.8 km). The bores were installed within 20 m of the river at 6–7 m depth below surface, with screened sections 1–1.5 m in length. Bores were sampled using an impeller pump set at the screened section and at least 3 bore volumes were pumped before samples were collected.

2.3 Sample preparation and analysis

Electrical conductivity (EC) was measured in the field using a calibrated TPS pH/EC meter. Water samples were preserved in the field by refrigeration in air-tight polyethylene bottles. Samples were filtered through 0.45 µ cellulose nitrate filters and analysed for anions using a Metrohm ion chromatograph at Monash University, Clayton; precision estimated by replicate analysis is ±2 %. Filtered samples were acidified to pH < 2 using twice-distilled 16 M nitric acid and analysed for cations by Varian Vista ICP-AES

HESSD
10, 3795–3842, 2013

at the Australian National University or at Monash University, Clayton, using a Thermo Finnigan X series II, quadrupole ICP-MS. Drift during ICP-MS analysis was corrected using internal Sc, Y, In, Bi standards and replicate analyses indicate a precision of ±5 %. The activity of ^{222}Rn in water samples was measured using a RAD-7 radon-in-air detector by the method outlined in Burnett and Dulaiova (2006) and is reported in $\mathrm{Bq\,m^{-3}}$. ^{222}Rn was degassed from 500 mL of water for 5 min into an air tight loop of a known volume. Total counting times were 2 h for surface water and 40 min for groundwater. Uncertainties based on replicate analyses are less than 15 % for ^{222}Rn activities below 1000 $\mathrm{Bq\,m^{-3}}$ and less than 5 % for ^{222}Rn activities above 1000 $\mathrm{Bq\,m^{-3}}$. Streambed sediments were sampled at 20.0 km on the Tambo River for ^{222}Rn ingrowth experiments. Four sediment samples of approximately 1.45 kg were allowed to equilibrate with ~ 500 mL of Ra free water for 8 weeks, before 150 mL of water was sampled for ^{222}Rn analysis using the methods outlined above.

2.4 Mass balance calculations

Assuming that both the concentration of ^{222}Rn in the atmosphere and the ingrowth of ^{222}Rn in river water through the decay of ^{226}Ra in suspended sediment are negligible (Cook et al., 2006; Mullinger et al., 2007), the inflow of groundwater (I in $\mathrm{m^3\,m^{-1}\,day^{-1}}$) may be calculated from changes in ^{222}Rn activity in the river c_r ($\mathrm{Bq\,m^{-3}}$) with distance x (m) by:

$$I = \left(Q\frac{\mathrm{d}c_\mathrm{r}}{\mathrm{d}x} - wEc_\mathrm{r} - F_\mathrm{h} + kdwc_\mathrm{r} + \lambda dwc_\mathrm{r}\right) / (c_i - c_\mathrm{r}) \quad (2)$$

(Cartwright et al., 2011; Cook et al., 2006), where Q is river discharge ($\mathrm{m^3\,day^{-1}}$), w is stream width (m), E is the evaporation rate ($\mathrm{m\,day^{-1}}$), F_h is the flux of ^{222}Rn from the hyporheic zone ($\mathrm{Bq\,m^{-1}\,day^{-1}}$), k is the gas transfer constant ($\mathrm{day^{-1}}$), d is river depth (m), λ is the radon decay constant (0.181 $\mathrm{day^{-1}}$) and c_i is the activity of ^{222}Rn in groundwater ($\mathrm{Bq\,m^{-3}}$). The hyporheic zone can be defined as the part of the surface

HESSD
10, 3795–3842, 2013

Groundwater – surface water interactions

N. P. Unland et al.

aquifer adjacent to the river that exchanges water with the river over relatively short distances and timescales (Boano et al., 2007; Kasahara and Wondzell, 2003). The net flux of ^{222}Rn from the hyporheic zone can be represented by:

$$F_h = q_h(c_h - c_r) \quad (3)$$

(Cook et al., 2006) where q_h is the volumetric flux from the hyporheic zone in $m^3\,day^{-1}$ (assuming a net flux of 0) and c_h is the activity of ^{222}Rn in the hyporheic zone (assuming a single well mixed reservoir). While c_h is simple to measure in the field, calculating q_h has historically been solved by conducting in stream tracer injections and modelling breakthrough curves (Wagner and Harvey, 1997; Runkel, 1998), which can be logistically difficult in large river systems. The flux of ^{222}Rn from the hyporheic zone can alternatively be estimated from river stretches that are not receiving groundwater input where there is no change in ^{222}Rn (Cartwright et al., 2011). If $dc_r/dx = 0$ and $I = 0$, F_h may be estimated from Eq. (2) as:

$$F_h = kdwc_r + \lambda dwc_r - wEc_r \quad (4)$$

Gas transfer rates (k) were estimated using the O'Connor and Dobins (1958) and Negulescu and Rojanski (1969) gas transfer models as modified by Genereux and Hemond (1992) and Mullinger et al. (2007):

$$k = 9.301 \times 10^{-3} \left(\frac{v^{0.5}}{d^{1.5}}\right) \quad (5)$$

and

$$k = 4.87 \times 10^{-4} \left(\frac{v}{d}\right)^{0.85} \quad (6)$$

where d is river depth (m) and v is stream velocity ($m\,day^{-1}$) as calculated from discharge, depth and width data.

HESSD
10, 3795–3842, 2013
Groundwater – surface water interactions
N. P. Unland et al.

A mass balance approach may also be used to estimate groundwater inflows from changes in the concentration of major ions, such as Cl. For a conservative ion such as Cl, mass balance calculations are simplified as decay, degassing and hyporheic flux terms are removed. Thus Eq. (2) reduces to

$$I = \left(Q\frac{\mathrm{dCl}_r}{\mathrm{d}x} - wE\,\mathrm{Cl}_r\right) / (\mathrm{Cl}_i - \mathrm{Cl}_r) \tag{7}$$

where Cl_i and Cl_r are the concentrations of Cl in the groundwater and river, respectively.

3 Results

3.1 ^{222}Rn activities

Figure 3 summarises the ^{222}Rn activities from all sampling campaigns on the Tambo River. These range from 52–604 Bq m^{-3} and show significant spatial and temporal variation. The average activity of ^{222}Rn in the Tambo River during April 2010 was 235 Bq m^{-3}, with elevated activities between 31.5 km and 28.5 km (> 450 Bq m^{-3}) and from 16.2 km to 13.8 km (> 330 Bq m^{-3}). While ^{222}Rn activities were generally lower in September 2010 (average = 180 Bq m^{-3}), elevated activities were again observed at 28.5 km (256 Bq m^{-3}) and 16.2 km (373 Bq m^{-3}). ^{222}Rn activities in February 2011 were also elevated at 28.5 km (263 Bq m^{-3}) but not at 16.2 km. Instead, a secondary increase ^{222}Rn activity occurred between 13.8 km and 10.4 km, with activities increasing to 468 Bq m^{-3} and 604 Bq m^{-3}, respectively.

Average ^{222}Rn activities in April 2011 were the lowest of any campaign (160 Bq m^{-3}) with increased activities between 28.5 km and 25.6 km (from 145 to 251 Bq m^{-3}) and between 18.6 km and 13.8 km (from 103 to 232 Bq m^{-3}). Average ^{222}Rn activities during August 2011 were the highest of any campaign (380 Bq m^{-3}), ranging from 236 to 554 Bq m^{-3}. Trends during this period were less apparent; however increased ^{222}Rn

HESSD
10, 3795–3842, 2013

activities still occurred between 31.5 and 28.5 km (from 263 to 348 $\mathrm{Bq\,m^{-3}}$) and between 20.0 and 13.8 km (from 358 to 546 $\mathrm{Bq\,m^{-3}}$). The distribution of ^{222}Rn activities in March is similar to that given by the average over all sampling periods (Fig. 3), with ^{222}Rn activities increasing from 63 $\mathrm{Bq\,m^{-3}}$ at 40.4 km to 210 $\mathrm{Bq\,m^{-3}}$ at 28.5 km, and from 142 $\mathrm{Bq\,m^{-3}}$ at 20.0 km to 236 $\mathrm{Bq\,m^{-3}}$ at 13.8 km. Spatially, the lowest ^{222}Rn activities in the Tambo River occurred between 1.8 km and the mouth of the Tambo River, with an average activity of 106 $\mathrm{Bq\,m^{-3}}$ over all campaigns.

^{222}Rn activities in the Nicholson River were generally lower than those in the Tambo River, with 16 of the 27 samples recording activities below 120 $\mathrm{Bq\,m^{-3}}$. During April and September 2010, ^{222}Rn activities in the Nicholson River were < 100 $\mathrm{Bq\,m^{-3}}$ at all sites except 13.6 km, which had activities of 370 and 734 $\mathrm{Bq\,m^{-3}}$, respectively (Fig. 4). In February 2011 activities were < 200 $\mathrm{Bq\,m^{-3}}$ for all sites except at 3.2 km which had an activity of 856 $\mathrm{Bq\,m^{-3}}$. Activities varied little during April 2011, with all activities below 120 $\mathrm{Bq\,m^{-3}}$. In August 2011 and March 2012, activities were < 200 $\mathrm{Bq\,m^{-3}}$ at all sites except the uppermost sample point (21.2 km), in which activities were 891 and 292 $\mathrm{Bq\,m^{-3}}$, respectively.

Groundwater ^{222}Rn activities at Location 1 ranged from 2380 to 9330 $\mathrm{Bq\,m^{-3}}$, with an average activity of 5000 $\mathrm{Bq\,m^{-3}}$ over the study period. Activities at this site were generally higher in February and April 2011 (avg. = 6790 $\mathrm{Bq\,m^{-3}}$) than during August 2011 and March 2012 (avg. = 3500 $\mathrm{Bq\,m^{-3}}$). Groundwater activities at Location 2 were generally lower than Location 1, ranging from 170 to 4240 $\mathrm{Bq\,m^{-3}}$ with an average activity of 1650 $\mathrm{Bq\,m^{-3}}$. Groundwater activities at Location 3 were the highest of any site, with an average activity of 8740 $\mathrm{Bq\,m^{-3}}$ over the study, ranging from 13 480 $\mathrm{Bq\,m^{-3}}$ in August 2011 to 5220 $\mathrm{Bq\,m^{-3}}$ in March 2012. The activity of ^{222}Rn in water equilibrated with streambed sediments ranged from 1900 to 3740 $\mathrm{Bq\,m^{-3}}$, with an average of 2600 $\mathrm{Bq\,m^{-3}}$. These are similar to that given by averaging Location 1 and Location 2 activities during sampling campaigns, which ranged from 2320 to 4600 $\mathrm{Bq\,m^{-3}}$.

HESSD
10, 3795–3842, 2013

Groundwater – surface water interactions

N. P. Unland et al.

3.2 River gauging and water elevation

The parameters used to calculate groundwater fluxes Q_f using Eq. (1) are listed in Table 1. The discharge of the Tambo River at the Battens Landing station varied by up to two orders of magnitude during the study, ranging from 6.6×10^4 m^3 day^{-1} in April 2010 to 7.9×10^6 m^3 day^{-1} in August 2011. Direct rainfall to the river for the 48 h period leading up to and including sampling/analysis ranged from 0 to 4093 m^3 day^{-1}. Direct evaporative losses for the same periods were on a similar order of magnitude as rainfall, ranging from 636 to 1974 m^3 day^{-1} and averaging 1190 m^3 day^{-1}.

River elevation (relative to the Australian Height Datum, AHD) during the February 2011 survey decreased from 6.66 to −0.15 m between 31.5 km and 18.1 km with a slope of ∼ 0.46 m km^{-1}. From 30.5 to 30.0 km and 29.5 to 29.2 km, the gradient of the river is higher than average: ∼ 1.1 and ∼ 0.79 m km^{-1}, respectively (Fig. 5). Conversely, between 24.7 and 23.7 km the gradient of the river slope is ∼ 0.2 m km^{-1}. Between 18.1 and 7.7 km river elevation changed very little, ranging from 0.26 to −0.15 m, with an average elevation of −0.01 m. Groundwater elevations neighbouring the Tambo River were the highest in August 2011 ranging from 8.86 m at Location 1 to 3.63 m at Location 3. Elevations were the lowest in April 2011 ranging from 7.51 m at Location 1 to 3.15 m at Location 3. Groundwater–surface water gradients at Location 1 were towards the Tambo River (positive) in all campaigns except August 2011, ranging from −0.018 (August 2011) to 0.112 (March 2012), with an average gradient of 0.027 (Fig. 5). Gradients at Location 2 were towards the river during all campaigns, ranging from 0.001 in August 2011 to 0.075 March 2012, with an average gradient of 0.033. The gradient at Location 3 in February was 0.013.

3.3 Temperature and EC surveys

The results of the temperature/EC surveys on the Tambo River are summarised in Fig. 5. River water temperature in February ranged from 21.6 °C at 31.5 km to 25.0 °C at 7.7 km (Fig. 5). Groundwater temperatures near the Tambo River at this time were

HESSD
10, 3795–3842, 2013

~ 15.5 °C at Location 1, increasing to ~ 16.5 °C at Location 3. While downstream increases in river temperature were generally gradual between 31.5 km and 15.6 km (with a gradient of ~ 0.11 °C km^{-1}), a number of stretches were not consistent with this trend. Between 29.9 km and 28.7 km temperature remained at ~ 20.0 °C, while an increase in temperature from 22.3 °C to 22.7 °C occurred between 26.9 km and 25.8 km. Between 24.8 km and 24.0 km temperature declined from 22.8 °C to 22.5 °C, while sharp increase in temperature (from 22.9 °C to 23.6 °C) occurred at ~ 21.4 km. Between 20.5 km and 18.9 km temperature did not show a systematic increase, varying between 23.2 °C and 23.1 °C. Downstream of 15.6 km the Tambo River was estuarine and temperatures were more variable ranging from 23 °C to 25 °C, with a drop in temperature of > 1.0 °C between 13.2 km and 11.8 km.

The EC of river water in February ranged from 112–9270 µS cm^{-1} with a sharp increase from 120 to 645 µS cm^{-1} between 16 and15 km, indicating the mixing of fresh water with estuarine water. Electrical conductivities changed very little from 31.5 to 15 km (114–150 µS cm^{-1}) and increased variably to > 9270 µS cm^{-1} downstream of 15 km. The electrical conductivity of groundwater near the Tambo River during February 2011 ranged from 145–260 µS cm^{-1} at Location 1, from 2200 to 2400 µS cm^{-1} at Location 2 and was ~ 7080 µS cm^{-1} at Location 3.

Groundwater temperatures in March 2012 were less variable than February 2011, increasing from ~ 15.3 °C at Location 1 to ~ 15.5 °C at Location 3. River temperature at this time was also less variable, ranging from 18.4 °C to 20.1 °C. River temperature remained at ~ 18.5 °C between 30.1 km and 29.2 km (Fig. 5), before increasing rapidly and irregularly to 19.6 °C between 29.2 and 25.5 km. Temperatures then declined to 19.4 °C between 25.5 and 24.3 km. Temperatures varied little between 24.3 km and 21.1 km (19.5 ± 0.1 °C), with an increase to 19.8 °C between 21.1 and 20.3 km. Temperatures were again relatively constant (19.8 ± 0.1 °C) between 20.5 and 15.8 km. Downstream of 15.8 km temperature increased variably as the river became estuarine, with an initial drop in temperature to 18.8 °C between 13.7 and 11.7 km.

EC values of the Tambo River during March 2012 ranged from 141–338 µS cm^{-1} between 40.4 and 20.1 km. The EC of groundwater near the Tambo River during March 2012 ranged from 140–290 µS cm^{-1} at Location 1, from 1650 to 1850 µS cm^{-1} at Location 2 and was 3410 µS cm^{-1} at Location 3. River electrical conductivities at this time varied from 148–195 µS cm^{-1} between 31.5 and 16 km on the Tambo River and increased variably to 338 µS cm^{-1} downstream of 16 km.

3.4 Chloride concentrations

Downstream trends in Cl concentrations on the Tambo River are similar to trends in EC from the EC/temperature surveys (Fig. 6), with lower variability between 40.4 km and 20.0 km followed by abrupt increases as the river becomes estuarine downstream of 20.0 km. Between 40.4 km and 20.0 km, Cl concentrations ranged from 13.4–18.9 mg L^{-1} in April 2010, 8.6–9.8 mg L^{-1} in September 2010, 8.9–9.8 mg L^{-1} in February 2011, 3.6–4.1 mg L^{-1} in April 2011, 18.0–19.6 mg L^{-1} in August 2011 and 18.0–19.6 mg L^{-1} in March 2012. Increases downstream of this were greater, reaching 10 650 mg L^{-1} at 16.2 km in April 2010. Similar trends were observed at 16.2 km during February 2011 and April 2011, with Cl concentrations increasing to 6322 mg L^{-1} and 266 mg L^{-1}, respectively. Changes in Cl concentrations during September 2010, August 2011 and March 2012 were more gradual, increasing from 11.1 mg L^{-1} to 9712 mg L^{-1}, 19.3 mg L^{-1} to 4030 mg L^{-1} and 23.0 mg L^{-1} to 10 334 mg L^{-1}, respectively, between 18.6 km and Lake King.

Similar to the Tambo River, the Nicholson River showed large, abrupt downstream increases in Cl concentrations during most sampling campaigns (Fig. 7). In April 2010 this occurred between 21.2 km and 15.3 km, increasing from 15.1 mg L^{-1} to 4947 mg L^{-1}. In September 2010, February 2011 and April 2011 this occurred further downstream (between 15.3 km and 13.6 km), with concentrations increasing from 25.6 to 2261 mg L^{-1}, 92.7 to 2632 mg L^{-1} and 10.0 to 102.7 mg L^{-1}, respectively. During March 2012 this increase occurred even further downstream, with concentrations

HESSD
10, 3795–3842, 2013

reaching 276 mg L^{-1} at 3.2 km. During August 2011, Cl concentrations only exceeded 100 mg L^{-1} at Lake King.

Cl concentrations in groundwater at Location 1 were the highest during March 2012, ranging from 17.8 to 23.4 mg L^{-1} and averaging 20.6 mg L^{-1}. Cl concentrations at this location were the lowest during April 2011, ranging from 6.75 to 10.3 mg L^{-1} with an average of 8.53 mg L^{-1}. Concentrations at Location 2 were significantly higher than Location 1, with concentrations ranging between 385 mg L^{-1} and 599 mg L^{-1} over the study. Average concentrations at Location 2 were the highest in February 2011 (563 mg L^{-1}) and the lowest in March 2012 (464 mg L^{-1}). Concentrations at location 3 were again higher, ranging from 474 mg L^{-1} in April 2011 to 598 mg L^{-1} in March 2012.

3.5 Groundwater fluxes

3.5.1 ^{222}Rn mass balance

The flux of groundwater to the Tambo and Nicholson Rivers was calculated using Eq. (2). River discharge (Q) for the Tambo River was based on interpolation between discharge values at the Ramrod Creek (40.4 km) and Battens Landing (20 km) gauging stations, while Q for the Nicholson River uses the discharge at the Sarsfield gauging station at 15.3 km. As river discharge will vary tidally throughout the estuarine sections of these rivers and river gauging does not occur in these reaches, groundwater fluxes were not calculated where EC data indicates estuarine conditions. Calculations are based on the average ^{222}Rn activity of groundwater (C_i) measured in each sampling round at Locations 1 and 2 (total = 5 bores). These bores are located in the upstream reaches for which groundwater fluxes have been calculated and sediment ingrowth experiments yielded ^{222}Rn activities within the range of those in groundwater at these locations.

Groundwater fluxes for a given reach are calculated using the average depth, width and gas transfer velocities for that reach. The flux of ^{222}Rn from the hyporheic zone (F_h) of the Tambo River was estimated using Eq. (4) when groundwater fluxes (I)

of 0 were calculated by Cl and ^{222}Rn mass balance between 21.9 km and 20.0 km in February 2011 (Fig. 9). At this time dc_r/dx was ~ 0, k was 1.16 m day^{-1}, E was 5×10^{-3} m day^{-1} (Bureau of Meteorology, 2012) and C_r was 150 Bq m^{-3}, giving a flux of 5440 Bq m^{-1} day^{-1}. The same was done for the Nicholson River during the April 2011 sampling period, when dc_r/dx was ~ 0 between 13.6 and 3.2 km, giving an I of 0 m^3 m^{-1} day^{-1} by Cl and ^{222}Rn mass balance. At this time k was 0.1 m day^{-1}, E was 5×10^{-3} m day^{-1} and C_r was 102 Bq m^{-3}, yielding a flux of 7610 Bq m^{-1} day^{-1}. The river morphology and stream bed sediment of these sections are representative of the Tambo and Nicholson Rivers and thus, likely to accurately represent F_h to the rivers. It is possible however that F_h will vary over time and location as a function of river slope and I. The uncertainties associated with fluxes of ^{222}Rn from the hyporheic zone are discussed in Sect. 4.2.

Between April 2010 and April 2011, groundwater fluxes between 40.4 and 18.6 km ranged from 0 to 3.3 m^3 m^{-1} day^{-1}, with an average total groundwater discharge to the section of 17 300 m^3 day^{-1} (Fig. 8). During this period groundwater fluxes were relatively high at 28.5 km, with an average flux of 1.56 m^3 m^{-1} day^{-1}. In contrast, fluxes between 21.8 km and 20.0 km were 0 m^3 m^{-1} day^{-1} for all sampling periods between April 2010 and April 2011, excluding February 2011 when fluxes were 0.78 m^3 m^{-1} day^{-1}. Groundwater fluxes under higher flow conditions in August 2011 and March 2012 ranged from 0–80.1 m^3 m^{-1} day^{-1} with an average total groundwater discharge of 320 000 m^3 day^{-1} to the study stretch. While groundwater fluxes during March 2012 were again the highest at 28.5 km (15.32 m^3 m^{-1} day^{-1}), groundwater fluxes during August were the highest at 21.9 km (80.1 m^3 m^{-1} day^{-1}). The cumulative groundwater discharge to the study section of the Tambo River was higher during August 2011 and March 2012 (535 000 and 20 100 m^3 day^{-1}), representing 12.7 % and 8.2 % of total river flow, respectively. During intermediate flow conditions from September 2010 to April 2011, groundwater constituted less than 10.0 % of river discharge, while groundwater discharge represented 21.4 % of total river discharge under the lowest flow conditions in April 2010.

HESSD
10, 3795–3842, 2013

As the Nicholson River was subject to tidal forcing in the study section during April 2010 and February 2011, groundwater fluxes were not calculated for these periods. The cumulative volume of groundwater discharged to the study stretch of Nicholson River was significantly lower than the Tambo River, ranging from 88.4 $m^3 day^{-1}$ in April 2011 to 32 900 $m^3 day^{-1}$ in August 2012. Similar to the Tambo River, a relatively high proportion of river flow (18.9 %) was sustained by groundwater discharge under low flow conditions in September 2010. Groundwater contributions to the Nicholson River were the lowest under intermediate flow conditions during April 2011, at < 1 % of total river discharge. Analogous to the Tambo River, groundwater contributes a significant proportion of total river discharge under the highest flow conditions in August 2011 and March 2012, representing 10.9 % and 14.9 % of total river discharge, respectively.

3.5.2 Cl mass balance

Groundwater fluxes were estimated from Cl concentrations using Eq. (7). Groundwater fluxes were only calculated for the upstream reaches in which estuarine water did not impact river Cl concentrations. Cl mass balance calculations for the Tambo River are based on the average Cl concentrations of groundwater from Locations 1 and 2, which ranged from 228–253 $mg L^{-1}$. For the Nicholson River, Cl mass balance could only be conducted between 21.2 km and 13.5 km for all periods except August 2011. In the absence of groundwater data neighbouring the Nicholson River, groundwater Cl data from the Tambo River has been used. Concentrations from Location 2 have been used as these are most likely to reflect the concentrations of groundwater neighbouring the Nicholson River (see Sect. 4.2).

Cl mass balance gave groundwater fluxes ranging from 0 to 4.85 $m^3 m^{-1} day^{-1}$ between sampling points on the Tambo River. These were generally higher between 21.9 and 20.0 km, averaging 1.17 $m^3 m^{-1} day^{-1}$. The total groundwater discharge by Cl mass balance was the highest in March 2012 (14 800 $m^3 day^{-1}$) and the lowest in April 2011 (522 $m^3 day^{-1}$) (Fig. 9). Groundwater constituted the highest proportion of

HESSD
10, 3795–3842, 2013

Groundwater – surface water interactions

N. P. Unland et al.

river discharge in April 2010 (2.4 %) and the lowest under intermediate flow conditions in September 2010 (0.61 %).

Cl mass balance calculations indicate that groundwater discharge to the Nicholson River was higher during August 2011 (38 300 $m^3\,day^{-1}$) and September 2011 (20 900 $m^3\,day^{-1}$), and lower during September 2010 (4810 $m^3\,day^{-1}$) and March 2012 (3960 $m^3\,day^{-1}$). Groundwater discharge represented the highest proportion of river flow under low flow conditions during September 2010 at 29.4 %, compared to high flow conditions in August 2011 and March 2012 in which groundwater constituted less than 7 % of total river flow.

4 Discussion

This section focuses on combining chemical and physical methods in order to characterise the distribution of gaining and loosing reaches along the Tambo and Nicholson Rivers. The impact of changing meteorological and hydrological conditions as drivers of groundwater fluxes is also investigated. Finally the discrepancies, strengths and weaknesses of different methods are discussed.

4.1 Spatial variability of groundwater discharge to the Tambo River

As groundwater temperatures near the Tambo River were lower than river temperatures during the temperature surveys, decreases in river temperature are likely to indicate increased groundwater discharge, while increased river temperature is likely to indicate reduced groundwater discharge (e.g. Becker et al., 2004). Temperature along the Tambo River in both surveys increased steadily between 31.5 and 27.0 km except for a zone at ~29 km where water temperature did not increase (Fig. 5), suggesting increased groundwater discharge. Average ^{222}Rn activities in this area are the second highest (302 $Bq\,m^{-3}$) of any sample location on the Tambo River yielding an average groundwater flux of 12.1 $m^3\,m^{-1}\,day^{-1}$. Furthermore, groundwater–surface water

HESSD
10, 3795–3842, 2013

gradients nearby at Location 1 were towards the river (6.1×10^{-3} to 0.112) during all periods except August 2011, supporting the gaining nature of this stretch. River elevation through this stretch is 5–10 m while areas within 200 m of the river are over 80 m in elevation (Fig. 10). Such areas of increased topography can facilitate greater groundwater head gradients (Sophocleous, 2002) and may account for the higher groundwater flux estimates, positive head gradients and temperature effects observed.

A decrease in groundwater discharge between 27 and 25.5 km is indicated by a general decline in ^{222}Rn activities and an average groundwater flux of 0.89 $m^3\,m^{-1}\,day^{-1}$ for the stretch. This is supported by an increase in temperature from 22.3–22.7 °C between 26.8 and 25.8 km in February 2011 and from 19.1–19.6 °C between 26.8 and 25.4 km in March 2012. As this stretch is neighboured by floodplains that extend for ~2 km in all directions (Fig. 2), the potential for large groundwater head gradients and groundwater influxes in the area is reduced. Conversely, as the Tambo River nears an area of increased topography at ~25 km, a decrease in river temperature over ~1 km is observed both in February 2011 (0.3 °C) and March 2012 (0.2 °C), suggesting increased groundwater discharge. This is supported by an increase in the average groundwater flux calculated by ^{222}Rn mass balance to 14.8 $m^3\,m^{-1}\,day^{-1}$.

A similar trend is observed between ~21 km and ~19 km. Through this reach, a sharp increase in river temperature (February 2011 = 22.9–23.6 °C, March 2012 = 19.5–19.8 °C) around 21 km suggests an area of reduced groundwater discharge (Fig. 5). This is followed by a section of relatively stable river temperature from ~20 km to 19 km (February 2011 = 23.2–23.1 °C, March 2012 = 19.9–19.7 °C), suggesting an increase in groundwater discharge. This is supported by ^{222}Rn mass balance which gives an average groundwater flux of 0.13 $m^3\,m^{-1}\,day^{-1}$ between 21.9 and 20 km, followed by an average flux of 23.5 $m^3\,m^{-1}\,day^{-1}$ between 20 and 18.6 km. The distribution of groundwater discharge through this reach again appears to be linked to the local topographic variation, with wider floodplains neighbouring the section of reduced groundwater discharge and greater topographic variation neighbouring the area of increased groundwater discharge (Fig. 10).

HESSD
10, 3795–3842, 2013

Between ~16 and 6.5 km, EC values increased to > 23 000 $\mu S\,cm^{-1}$ in February 2011 and > 300 $\mu S\,cm^{-1}$ in March 2012, indicating the transition into an estuarine setting. In this zone, mixing with warmer lake water (25–30 °C, Arnott and McKinnon, 1985) is expected to cause an increase in river temperature; however river temperature declines between 13.5 and 11.5 km, suggesting a zone of increased groundwater discharge. Nevertheless, mixing between lake water and river water through the estuarine fringe is not always systematic (e.g. MacKay and Schumann, 1990; Nunes Vaz et al., 1989; Stacey et al., 2008), and the decline in river temperature may be an artefact of measuring different water types as they mix variably through the estuarine fringe. While river discharge is not constrained through this reach preventing mass balance calculations, the average ^{222}Rn activity through this zone are the highest of any location on the Tambo River (324 $Bq\,m^{-3}$), supporting an increase in groundwater discharge. At 13.8 km the Tambo River is immediately adjacent to a cliff > 40 m in elevation. This may again facilitate high groundwater gradients toward the river resulting in higher groundwater inputs. While ^{222}Rn activities at 13.8 km were the highest of any sample location on the Tambo River, they were also highly variable (135–526 $Bq\,m^{-3}$). This variability may reflect the transient nature of the interface between river water and lake water as they mix under tidally driven flow conditions. Furthermore, changing river flow in estuaries over tidal cycles may affect the balance of ^{222}Rn at the estuarine fringe (Santos et al., 2010). Constraining such balances requires further work and is beyond the scope of this paper. While the tidal nature of the lower sections prevents mass balance calculations, a decline in ^{222}Rn activities through such reaches suggests reduced groundwater fluxes in the estuary. Lower topographic variation through this section (Fig. 10) will again provide less potential for the formation of high groundwater gradients. This is consistent with topographic variation as a driver of groundwater discharge to the Tambo River as asserted above.

HESSD
10, 3795–3842, 2013

4.2 Uncertainty analysis

The impact of uncertainties in k on groundwater discharge estimates using ^{222}Rn mass balance calculations was investigated by comparing alternate k values from Eqs. (5) and (6). The Negulescu and Rojanski model generally yields higher k values (and hence results in higher calculated groundwater fluxes) than the O'Connor and Dobins model, although this is reversed at low velocities and shallow depths (Fig. 11). This is demonstrated by the cumulative groundwater discharge estimates to the Tambo River, which were higher using Eq. (5) under low flow conditions during April 2010 and February 2011, but lower during higher flow coditions from other sampling periods. This trend is less apparent for the Nicholson river as river velocity is less variable and greater changes in river width and depth downstream have a greater impact on the equations. The difference in the cumulative groundwater discharge to the Nicholson River calculated using Eqs. (5) and (6) ranged from 3.1–44 % with an average difference of 20.1 %. For the Tambo River these differences ranged from 2.5–48 % with an average difference of 30 %. The varibility in k is recognised as a source of error in ^{222}Rn mass balance calculations, however it has very little impact the distribution of gaining reaches or seasonal trends in groundwater discharge identified by ^{222}Rn mass balance (Fig. 12).

For both the Tambo and Nicholson Rivers, F_h estimates were made when dc/dx was 0 (within 1 SD of the equipment precision). As the activity of ^{222}Rn in the Tambo and Nicholson Rivers is relatively low, failure to account for F_h will result in overestimations during groundwater flux calculations. On average, failure to account for F_h on the Tambo River resulted in a two fold increase in groundwater discharge. Excluding April 2011, failure to account for F_h on the Nicholson River results in an average increase in the estimated groundwater discharge by 45 %. As ^{222}Rn activities in the Nicholson are particularly low ($< 120\,\mathrm{Bq\,m^{-3}}$) at all locations during April 2011, failure to account for F_h at this time results in nearly a 4 fold increase in the groundwater discharge estimate. Unlike many other studies where F_h is ignored, this illustrates the need to account for

HESSD
10, 3795–3842, 2013

F_h in streams with lower ^{222}Rn activities where the dc_r/dx term in Eq. (2) is small (Cook et al., 2006).

The variability of C_i represents the greatest source of uncertainty in ^{222}Rn mass balance calculations as C_i values varied by up to 3 orders of magnitude at different locations. Due to the location of the C_i–C_r term in Eq. (2) and as $C_i \gg C_r$ during all sampling periods, a 50 % change in C_i will result in an approximate 50 % change in I. The sensitivity of the model to C_i is demonstrated by calculating I using the minimum and maximum C_i value measured during sampling periods. For example, by letting C_i = 329 Bq m^{-3} instead of 4620 Bq m^{-3} in February, a 50 fold increase in the groundwater discharge estimate to the Tambo River occurred. Conversely, when a C_i value of 9325 Bq m^{-3} is assigned for the same period, the groundwater discharge estimate is halved. While these are the most extreme C_i values and are unlikely to represent the actual activity of groundwater entering the Tambo River, this demonstrates the need to accurately assign groundwater end member values. The variability of ^{222}Rn activity in groundwater remains a source of uncertainty when conducting groundwater studies, and further research in characterising such variability both spatially and temporally would be useful to subsequent studies.

The sensitivity of the Cl mass balance model to Cl_i on the Tambo River was tested by assuming the Cl_i end member was a mixture between groundwater from Location 1 and 2, and then varying the weighting between each location. Using Location 2 concentrations as the end member reduced groundwater discharge estimates for the stretch by between 39 % and 40 % during individual sampling periods. Estimates using the Location 1 concentrations as the end member increased estimates by 2–4 orders of magnitude during September 2010, February 2011, April 2011 and March 2012 and reduced to 0 during April 2010 and August 2011 periods. For the Nicholson River, groundwater discharge estimates of 0 m^3 day^{-1} were given for all sampling periods when using Cl concentrations of Location 1. This is because the Cl_i at Location 1 is lower than Cl_r, meaning groundwater inputs would cause a decline in Cl_r in contrast to the observed increase in Cl_r. As such it is unlikely that groundwater entering the Nicholson River has similar Cl concentrations to bore 1, so those from bore 2 have been used. Cl_i again represents the greatest source of uncertainty in mass balance calculations given that values vary by up to 3 orders of magnitude between Locations 1 and 2. Furthermore, C_i is generally similar to C_r in upstream reaches, making Cl mass balance calculations very sensitive to variations in C_i, as opposed to ^{222}Rn mass balance calculations where $C_i \gg C_r$. This again highlights the need for accurate characterisation of groundwater end members.

4.3 Method comparison

While similar temporal trends in groundwater discharge to the Tambo River (i.e. increased groundwater discharge under high flow conditions) were identified by differential flow gauging, Cl mass balance and ^{222}Rn mass balance, estimates from Cl mass balance were generally 1–2 orders of magnitude lower than those from ^{222}Rn mass balance or differential flow gauging. This discrepancy is likely to partially reflect uncertainties in groundwater end-members and the sensitivity of the models to such uncertainties. Interaction between groundwater and surface water near rivers is likely to increase the variability of groundwater chemistry near rivers, making characterisation of the groundwater end member difficult (Lambs, 2004). Exchange at the river-groundwater interface is not uniform either spatially or temporally, and will vary according to river morphology, aquifer characteristics and changing flow conditions (Lambs, 2004; McCallum et al., 2010; Woessner, 2000). While this study used near river groundwater in an attempt to account for this variability, it is likely that spatial variations in groundwater–surface water interactions along the Tambo River remain unaccounted for.

Discrepancies may also reflect the discharge of relatively young groundwater that has only been stored for a period of weeks, either as recently infiltrated rainfall, bank return flow or parafluvial flow (McCallum et al., 2010; Woessner, 2000). Chemically, such groundwater would have low Cl concentrations but elevated ^{222}Rn activities through ingrowth over the storage period (Cartwright et al., 2011). This would result in higher

HESSD
10, 3795–3842, 2013
Groundwater – surface water interactions
N. P. Unland et al.

groundwater discharge estimates by ^{222}Rn mass balance compared to Cl mass balance; such as those observed on the Tambo River. Under these conditions, groundwater estimates from ^{222}Rn mass balance will more closely reflect the total volume of groundwater entering the river, whereas Cl mass balance will more closely reflect the volume of regional groundwater entering the river. This is likely to result in the observed correlation between differential flow gauging and ^{222}Rn mass balance, and the poor correlation between differential flow gauging and Cl mass balance (Fig. 13).

While there is a strong correlation between groundwater discharge estimates from ^{222}Rn mass balance and differential flow gauging, it is noted that estimates from ^{222}Rn mass balance are greater than those from differential flow gauging during April 2010 and April 2011. As ^{222}Rn mass balance will account for the total groundwater discharge, compared to differential flow gauging which accounts for the net groundwater discharge (inflow–outflow), this discrepancy may result from the presence of losing reaches. Sampling during April 2010 and April 2011 occurred after dry periods when the water table was low and losing reaches are more likely to occur. In contrast, groundwater discharge estimates during February 2011 given by differential flow gauging were greater than ^{222}Rn mass balance. This discrepancy is likely to reflect unaccounted for runoff during differential flow gauging as a result of increased rainfall in the catchment in the days leading up to sampling.

In contrast to the Tambo River, groundwater discharge to the Nicholson River estimated by Cl and ^{222}Rn mass balance were similar, ranging from 654 to 38 300 $m^3\,day^{-1}$ by Cl mass balance and from 88.4 to 61 100 $m^3\,day^{-1}$ by ^{222}Rn mass balance. This suggests that the groundwater end members used for mass balance calculations on the Nicholson River may more accurately characterise the groundwater entering the Nicholson River than the Tambo River. This suggests that groundwater–surface water interaction along the Nicholson River is less variable. Under such conditions, uncertainties associated with groundwater characterisation will be reduced.

This not only highlights the importance of accurately characterising groundwater chemistry when taking a mass balance approach, but emphasizes the need for

HESSD
10, 3795–3842, 2013

groundwater characterisation both regionally and at a high spatial resolution in areas proximal to river systems. This is because near river groundwater is (1) likely to be significantly different to regional groundwater, (2) will represent the chemistry of the water entering the river and (3) is likely to vary chemically both spatially and temporally when groundwater–surface water exchange is prevalent.

4.4 Hydrological drivers

Groundwater discharge to both the Tambo and Nicholson Rivers increased with river discharge. As sampling during high flow periods occurred in the days to weeks following peak flow conditions, sampling is likely to reflect a period in which river height is receding while groundwater levels are high. Under these conditions high groundwater gradients can form, resulting in increased groundwater discharge. These results indicate that during high rainfall periods, groundwater levels in the Tambo Catchment can increase fast enough to generate significant volumes of groundwater discharge (e.g. Cey et al., 1998). This is indicative of fast responding aquifers that are highly connected and conductive, and is consistent the Tertiary and Quaternary aquifers of the region that are dominated by coarse sands.

While the total groundwater discharge to the Tambo and Nicholson Rivers was the highest under high flow conditions, groundwater constituted the highest proportion of river flow under low flow conditions. For the Tambo River this occurred during April 2010, with groundwater discharge by ^{222}Rn mass balance representing 21.4 % of total river flow. For the Nicholson River, this occurred during September 2010, with groundwater discharge by ^{222}Rn mass balance constituting 18.9 % of river flow. Conversely, groundwater constituted the lowest proportion of river flow under intermediate flow conditions. This occurred during February 2011 on the Tambo River, with groundwater discharge by ^{222}Rn mass balance constituting 6.8 % of river discharge. For the Nicholson River this occurred during April 2011, with groundwater discharge by ^{222}Rn mass balance constituting < 1 % of river discharge. Both of these sampling campaigns took place during a time of increased rainfall (~ 35 mm of rainfall in the 4 days leading up

HESSD
10, 3795–3842, 2013

to sampling) that followed an extended dry period. As such, it is likely that these periods represent conditions in which the water table was still low while river levels were increasing due to runoff. This would result in low groundwater–surface water gradients and reduced groundwater discharge.

This study shows that while two rivers may vary significantly in their discharge (Tambo avg. $= 1.04 \times 10^6$ m^3 day^{-1}, Nicholson avg. $= 2.22 \times 10^5$ m^3 day^{-1}), groundwater discharge may vary on a similar scale (Tambo avg. $= 1.18 \times 10^5$ m^3 day^{-1}, Nicholson avg. $= 2.43 \times 10^4$ m^3 day^{-1}), resulting in similar groundwater components in both rivers. Furthermore, when two rivers occur in the same aquifer system, they are likely to respond similarly under changing rainfall and flow conditions; with relatively low volumes of groundwater providing a high proportion of river discharge under base flow conditions, rainfall and runoff providing a higher proportion of river discharge during increased rainfall following dry periods, and higher volumes of groundwater representing an intermediate proportion of river flow in the weeks following extensive rainfall in the catchment. This suggests that the lower discharge volumes associated with the Nicholson River are likely to represent the smaller catchment area from which its flow is derived, as opposed to differences in groundwater–surface water interaction.

5 Conclusions

By combining the use of chemical and physical tracer methods on the Tambo River, increased groundwater influx was identified near areas of increased topographic variation, where the potential for higher groundwater–surface water gradient formation is increased. The flux and total discharge of groundwater to the Tambo and Nicholson rivers was calculated using ^{222}Rn mass balance, Cl mass balance, and differential flow gauging. The highest volume of groundwater discharge occurred in the days to weeks following heavy rainfall, when river levels were receding and groundwater levels remained high. Groundwater formed the highest proportion of river discharge under baseflow conditions, while rainfall and runoff formed a higher proportion of river flow

HESSD
10, 3795–3842, 2013

during periods of increased rainfall that followed from dry periods in the catchment. Discrepancies between ^{222}Rn and Cl mass balance suggest that spatially variable bank exchange processes can amplify the heterogeneity of Cl in groundwater neighbouring rivers, while the equilibration between ^{222}Rn in aquifer sediments with groundwater can reduce the heterogeneity of ^{222}Rn in groundwater. Under these circumstances, extensive spatial groundwater sampling is required to accurately characterise the groundwater Cl end member. The impact of water exchange between rivers and groundwater on tracers at the bank scale is a process that is still poorly defined, and further investigation into these processes may prove particularly useful in the interpretation of tracer data during future groundwater–surface water studies.

Acknowledgements. We would like to thank Massimo Raveggi and Rachelle Pierson for their help with major ion analyses. Funding for this research was provided by the National Centre for Groundwater Reasearch and Training, and Australian Government initiative, supported by the Australian Research Council and the National Water Commission.

References

Anderson, M. P.: Heat as a ground water tracer, Ground Water, 43, 951–968, 2005.

Andersen, M. S. and Acworth, R. I.: Stream-aquifer interactions in the Maules Creek catchment, Namoi Valley, New South Wales, Australia, Hydrogeol. J., 17, 2005–2021, 2009.

Anibas, C., Fleckenstein, J. H., Volze, N., Bius, K., Verhoeven, R., Meire, P., and Batelaan, O.: Transient or steady-state? Using vertical temperature profiles to quantify groundwater–surface water exchange, Hydrol. Process., 23, 2165–2177, 2009.

Anibas, C., Buis, K., Verhoeven, R., Meire, P., and Batelaan, O.: A simple thermal mapping method for seasonal spatial patterns of groundwater–surface water interaction, J. Hydrol., 397, 93–104, 2011.

Arnott, G. H. and McKinnon, A. D.: Distribution and abundance of eggs of the anchovy, in relation to temperature and salinity in the Gippsland Lakes, Mar. Freshwater Res., 36, 433–439, 1985.

HESSD
10, 3795–3842, 2013

Becker, M. W., Georgian, T., Ambrose, H., Siniscalchi, J., and Fredrick, K.: Estimating flow and flux of ground water discharge using water temperature and velocity, J. Hydrol., 296, 221–233, 2004.

Boano, F., Revelli, R., and Ridolfi, L.: Bedform-induced hyporheic exchange with unsteady flows, Adv. Water Resour., 30, 148–156, 2007.

Boulton, A.: Stream ecology and surface-hyporheic hydrologic exchange: implications, techniques and limitations, Mar. Freshwater Res., 44, 553–564, 1993.

Bureau of Meteorology: Commonwealth of Australia, available at: http://www.bom.gov.au (last access: 11 January 2013), 2012.

Burnett, W. C. and Dulaiova, H.: Radon as a tracer of submarine groundwater discharge into a boat basin in Donnalucata, Sicily, Cont. Shelf Res., 26, 862–873, 2006.

Burnett, W. C., Peterson, R., Moore, W. S., and de Oliveira, J.: Radon and radium isotopes as tracers of submarine groundwater discharge – results from the Ubatuba, Brazil SGD assessment intercomparison, Estuar. Coast. Shelf S., 76, 501–511, 2008.

Cartwright, I., Weaver, T. R., and Tweed, S. O.: Integrating physical hydrogeology, hydrochemistry, and environmental isotopes to constrain regional groundwater flow: Southern Riverine Province, Murray Basin, Australia, in: International Association of Hydrogeologists Special Publication 11, Groundwater Flow Understanding from Local to Regional Scale, edited by: Carrillo, R. J. J. and Ortega, G. M. A., Taylor and Francis, London, UK, 10–134, 2008.

Cartwright, I., Weaver, T. R., Simmons, C. T., Fifield, L. K., Lawrence, C. R., and Chisari, R.: Physical hydrogeology and environmental isotopes to constrain the age, origins, and stability of a low-salinity groundwater lens formed by periodic river recharge: Murray Basin, Australia, J. Hydrol., 380, 203–221, 2010.

Cartwright, I., Hofmann, H., Sirianos, M. A., Weaver, T. R., and Simmons, C. T.: Geochemical and ^{222}Rn constraints on baseflow to the Murray River, Australia, and timescales for the decay of low-salinity groundwater lenses, J. Hydrol., 405, 333–343, 2011.

Cey, E. E., Rudolph, D. L., and Parkin, G. W., Aravena, R.: Quantifying groundwater discharge to a small perennial stream in southern Ontario, Canada, J. Hydrol., 210, 21–37, 1998.

Chaplin, H. J.: Eastern Victoria Water Table Aquifers, Groundwater Benificial Use Map Series, Department of Conservation and Natural Resources, available at: http://www.water.vic.gov.au/ (last access: 20 March 2013), 1995.

Corbett, D. R., Burnett, W. C., Cable, P. H., and Clark, S. B.: A multiple approach to the determination of radon fluxes from sediments, J. Radioanal. Nucl. Ch., 236, 247–252, 1998.

Cook, P. G.: Estimating groundwater discharge to rivers from river chemistry surveys, Hydrol. Process., online first, doi:10.1002/hyp.9493, 2012.
Cook, P. G., Favreau, G., Dighton, J. C., and Tickell, S.: Determining natural groundwater influx to a tropical river using radon, chlorofluorocarbons and ionic environmental tracers, J. Hydrol., 277, 74–88, 2003.
Cook, P. G., Lamontagne, S., Berhane, D., and Clark, J. F.: Quantifying groundwater discharge to Cockburn River, southeastern Australia, using dissolved gas tracers Rn-222 and SF_6, Water Resour. Res., 42, W10411, doi:10.1029/2006WR004921, 2006.
Cook, P. L. M., Holland, D. P., and Longmore, A. R.: Effect of a flood event on the dynamics of phytoplankton and biogeochemistry in a large temperate Australian lagoon, Limnol. Oceanogr., 55, 1123–1133, 2010.
Cox, M. H., Su, G. W., and Constantz, J.: Heat, Chloride, and Specific Conductance as Ground Water Tracers near Streams, Ground Water, 45, 187–195, 2007.
Department of Agriculture, Fisheries and Forrestry: available at: http://adl.brs.gov.au/water2010/pdf/catchment_223_0_summary.pdf (last access: 19 November 2012), 2006.
Durand, P., Neal, M., and Neal, C.: Variations in stable oxygen isotope and solute concentrations in small submediterranean montane streams, J. Hydrol., 144, 283–290, 1993.
Ellins, K. K., Roman-Mas, A., and Lee, R.: Using ^{222}Rn to examine groundwater/surface discharge interaction in the Rio Grande de Manati, Puerto Rico, J. Hydrol., 115, 319–341, 1990.
Genereux, D. P. and Hemond, H. F.: Naturally occurring Radon 222 as a tracer for streamflow generation: steady state methodology and field example, Water Resour. Res., 26, 3065–3075, 1990.
Genereux, D. P. and Hemond, H. F.: Determination of gas exchange rate constants for a small stream on Walker Branch Watershed, Tennessee, Water Resour. Res., 28, 2365–2374, 1992.
Genereux, D. P., Hemond, H. F., and Mulholland, P. J.: Use of radon-222 and calcium as tracers in a three-end-member mixing model for streamflow generation on the West Fork of Walker Branch Watershed, J. Hydrol., 142, 167–211, 1993.
Gilfedder, B. S., Hofmann, H., and Cartwright, I.: Novel instruments for in situ continuous Rn-222 measurement in groundwater and the application to river bank infiltration, Environ. Sci. Technol., 47, 993–1000, 2012.

HESSD
10, 3795–3842, 2013

Groundwater – surface water interactions

N. P. Unland et al.

Gonfiantini, R.: Environmental isotopes in lake studies, in: Handbook of Environmental Isotope Geochemistry, edited by: Fritz, P. and Fontes, J. C., 2. Elsevier Scientific, Amsterdam, Netherlands, 113–167, 1986.

Grayson, R. B., Gippel, C. J., Finlayson, B. L., and Hart, B. T.: Catchment-wide impacts on water quality: the use of "snapshot" sampling during stable flow, J. Hydrol., 199, 121–134, 1997.

Hallegraeff, G. M.: Harmful algal blooms in the Australian region, Mar. Pollut. Bull., 25, 186–190, 1992.

Harte, P. and Kiah, R.: Measured river leakages using conventional streamflow techniques: the case of Souhegan River, New Hampshire, USA, Hydrogeol. J., 17, 409–424, 2009.

Herczeg, A. L., Torgersen, T., Chivas, A. R., and Habermehl, M. A.: Geochemistry of ground waters from the Great Artesian Basin, Australia, J. Hydrol., 126, 225–245, 1991.

Hofmann, H., Gilfedder, B. S., and Cartwright, I.: A novel method using a silicone diffusion membrane for continuous ^{222}Rn measurements for the quantification of groundwater discharge to streams and rivers, Environ. Sci. Technol., 45, 8915–8921, 2011.

Isotope Hydrology Information System: The ISOHIS Database, available at: http://www.iaea.org/water/ (last access: 18 November 2012), 2012.

Jolly, R. L.: Bairnsdale, 1 : 250000 Geological Map Series, Department of Natural Resources and Environment, MDC Fitzroy, Victoria, 3065, 1997.

Kalbus, E., Reinstorf, F., and Schirmer, M.: Measuring methods for groundwater – surface water interactions: a review, Hydrol. Earth Syst. Sci., 10, 873–887, doi:10.5194/hess-10-873-2006, 2006.

Kasahara, T. and Wondzell, S. M.: Geomorphic controls on hyporheic exchange flow in mountain streams, Water Resour. Res., 39, 1005, doi:10.1029/2002WR001386, 2003.

Krause, S., Bronstert, A., and Zehe, E.: Groundwater – surface water interactions in a North German lowland floodplain – implications for the river discharge dynamics and riparian water balance, J. Hydrol., 347, 404–417, 2007.

Lambs, L.: Interactions between groundwater and surface water at river banks and the confluence of rivers, J. Hydrol., 288, 312–326, 2004.

Lamontagne, S. and Cook, P. G.: Estimation of hyporheic water residence time in situ using Rn-222 disequilibrium, Limnol. Oceanogr.-Meth., 5, 407–416, 2007.

Discussion Paper | Discussion Paper | Discussion Paper | Discussion Paper |

Lamontagne, S., Leaney, F. W., and Herczeg, A. L.: Groundwater-surface water interactions in a large semi-arid floodplain: implications for salinity management, Hydrol. Process., 19, 3063–3080, 2005.

Lamontagne, S., Le Gal La Salle, C., Hancock, G. J., Webster, I. T., Simmons, C. T., Love, A. J., James-Smith, J., Smith, A. J., Kämpf, J., and Fallowfield, H. J.: Radium and radon radioisotopes in regional groundwater, intertidal groundwater, and seawater in the Adelaide Coastal Waters Study area: implications for the evaluation of submarine groundwater discharge, Mar. Chem., 109, 318–336, 2008.

Lerner D, N., Issar A, S., and Simmers, I.: Groundwater recharge, a guide to understandin and estimating natural recharge, International Association of Hydrogeologists, Kenilworth, Rep 8, 1990.

Luc, L.: Interactions between groundwater and surface water at river banks and the confluence of rivers, J. Hydrol., 288, 312–326, 2004.

MacKay, H. M. and Schumann, E. H.: Mixing and circulation in the sundays river estuary, South Africa, Estuar. Coast. Shelf S., 31, 203–216, 1990.

Martens, C. S., Kipphut, G. W., and Klump, J. V.: Sediment-water chemical exchange in the coastal zone traced by in situ Radon-222 flux measurements, Science, 208, 285–288, 1980.

McCallum, J. L., Cook, P. G., Brunner, P., and Berhane, D.: Solute dynamics during bank storage flows and implications for chemical base flow separation, Water Resour. Res., 46, W07541, doi:10.1029/2009WR008539, 2010.

McCallum, J. L., Cook, P. G., Berhane, D., Rumpf, C., and McMahon, G. A.: Quantifying groundwater flows to streams using differential flow gaugings and water chemistry, J. Hydrol., 416, 118–132, 2012.

McCallum, A. M., Andersen, M. S., and Acworth R. I.: A new method for estimating recharge to unconfined aquifers using differential river gauging, Ground Water, in press, 2013.

Meredith, K. T., Hollins, S. E., Hughes, C. E., Cendón, D. I., Hankin, S., and Stone, D. J. M.: Temporal variation in stable isotopes (^{18}O and ^{2}H) and major ion concentrations within the Darling River between Bourke and Wilcannia due to variable flows, saline groundwater influx and evaporation, J. Hydrol., 378, 313–324, 2009.

Mullinger, N. J., Binley, A. M., Pates, J. M., and Crook, N. P.: Radon in Chalk streams: spatial and temporal variation of groundwater sources in the Pang and Lambourn catchments, UK, J. Hydrol., 339, 172–182, 2007.

Mullinger, N. J., Pates, J. M., Binley, A. M., and Crook, N. P.: Controls on the spatial and temporal variability of ^{222}Rn in riparian groundwater in a lowland Chalk catchment, J. Hydrol., 376, 58–69, 2009.
Négrel, P., Petelet-Giraud, E., Barbier, J., and Gautier, E.: Surface water–groundwater interactions in an alluvial plain: chemical and isotopic systematics, J. Hydrol., 277, 248–267, 2003.
Negulescu, M. and Rojanski, V.: Recent research to determine reaeration coefficients, Water Res., 3, 189–202, 1969.
Nunes Vaz, R. A., Lennon, G. W., and de Silva Samarasinghe, J. R.: The negative role of turbulence in estuarine mass transport, Estuar. Coast. Shelf S., 28, 361–377, 1989.
O'Connor, D. J. and Dobbins, W. E.: Mechanisms of reaeration in natural streams, T. Am. Soc. Civ. Eng., 123, 641–684, 1958.
Panno, S. V., Hackley, K. C., Hwang, H. H., Greenberg, S. E., Krapac, I. G., Landsberger, S., and O'Kelly, D. J.: Source identification of sodium and chloride in natural waters: preliminary results, Ground Water, 44, 176–187, 2006.
Peterson, R. N., Santos, I. R., and Burnett, W. C.: Evaluating groundwater discharge to tidal rivers based on a Rn-222 time-series approach, Estuar. Coast. Shelf S., 86, 165–178, 2010.
Peyrard, D., Delmotte, S., Sauvage, S., Namour, P. H., Gerino, M., Vervier, P., and Sanchez-Perez, J. M.: Longitudinal transformation of nitrogen and carbon in the hyporheic zone of an N-rich stream: a combined modelling and field study, Phys. Chem. Earth, 36, 599–611, 2011.
Rhode, A.: Spring flood: meltwater or groundwater?, Nord. Hydrol., 12, 21–30, 1981.
Ribolzi, O., Andrieux, P., Valles, V., Bouzigues, R., Bariac, T., and Voltz, M.: Contribution of groundwater and overland flows to storm flow generation in a cultivated Mediterranean catchment, quantification by natural chemical tracing, J. Hydrol., 233, 241–257, 2000.
Rau, G. C., Andersen, M. S., McCallum, A. M., and Acworth, R. I.: Analytical methods that use natural heat as a tracer to quantify surface water-groundwater exchange, evaluated using field temperature records, Hydrogeol. J., 18, 1093–1110, 2010.
Ruehl, C., Fisher, A. T., Hatch, C., Los Huertos, M., Stemler, G., and Shennan, C.: Differential gauging and tracer tests resolve seepage fluxes in a strongly-losing stream, J. Hydrol., 330, 235–248, 2006.
Santos, I. R. and Eyre, B. D.: Radon tracing of groundwater discharge into an Australian estuary surrounded by coastal acid sulphate soils, J. Hydrol., 396, 246–257, 2011.

Santos, I. R., Peterson, R. N., Eyre, B. D., and Burnett, W. C.: Significant lateral inputs of fresh groundwater into a stratified tropical estuary: evidence from radon and radium isotopes, Mar. Chem., 121, 37–48, 2010.
Silliman, S. E. and Booth, D. F.: Analysis of time-series measurements of sediment temperature for identification of gaining vs. losing portions of Juday Creek, Indiana, J. Hydrol., 146, 131–148, 1993.
Sophocleous, M.: Interactions between groundwater and surface water: the state of the science, Hydrogeol. J., 10, 52–67, 2002.
Stacey, M. T., Fram, J. P., and Chow, F. K.: Role of tidally periodic density stratification in the creation of estuarine subtidal circulation. J. Geophys. Res., 113, C08016, doi:10.1029/2007JC004581, 2008.
Stellato, L., Petrellz, E., Terrasi, F., Bellonie, P., Belli, M., Sansone, U., and Celico, F.: Some limitations in using ^{222}Rn to assess river–groundwater interactions: the case of Castel di Sangro alluvial plain (central Italy), Hydrogeol. J., 16, 701–712, 2008.
Tsur, Y. and Graham-Tomasi, T.: The buffer value of groundwater with stochastic surface water supplies, J. Environ. Econ. Manag., 21, 201–224, 1991.
Vandenberg, A. H. M. and Stewart, I. R.: Ordovician terranes of the southeastern Lachlan Fold Belt: stratigraphy, structure and palaeogeographic reconstruction, Tectonophysics, 214, 159–176, 1992.
Victorian Water Resources Data Warehouse: available at: http://www.vicwaterdata.net/vicwaterdata/home.aspx (last access: 11 January 2013), 2012.
Wagner, B. J. and Harvey, J. W.: Experimental design for estimating parameters of rate-limited mass transfer: analysis of stream tracer studies, Water Resour. Res., 33, 1731–1741, 1997.
Woessner, W. W.: Stream and fluvial plain ground water interactions: rescaling hydrogeologic thought, Ground Water, 38, 423–429, 2000.
Zhang, J., Letolle, R., Martin, J. M., Jusserand, C., and Mouchel, J. M.: Stable oxygen isotope distribution in the Huanghe (Yellow River) and the Changjiang (Yangtze River) estuarine systems, Cont. Shelf Res., 10, 369–384, 1990.

HESSD
10, 3795–3842, 2013

Groundwater – surface water interactions

N. P. Unland et al.

Table 1. Parameters used for calculating the net groundwater flux (Q_f) by differential flow gauging using Eq. (1).

Parameter	Apr 10	Sep 10	Feb 11	Apr 11	Aug 12	Mar 10
Q_u ($m^3 day^{-1}$)	60 473	305 115	152 516	188 493	7 328 592	1 249 945
Q_d ($m^3 day^{-1}$)	65 978	354 034	178 316	201 032	7 869 027	1 393 043
P ($m^3 day^{-1}$)	238	0	4093	3378	119	40
E ($m^3 day^{-1}$)	1033	1073	1974	636	636	1788
Q_f ($m^3 day^{-1}$)	6300	49 992	23681	9797	540 952	144 846

HESSD
10, 3795–3842, 2013
Groundwater – surface water interactions
N. P. Unland et al.

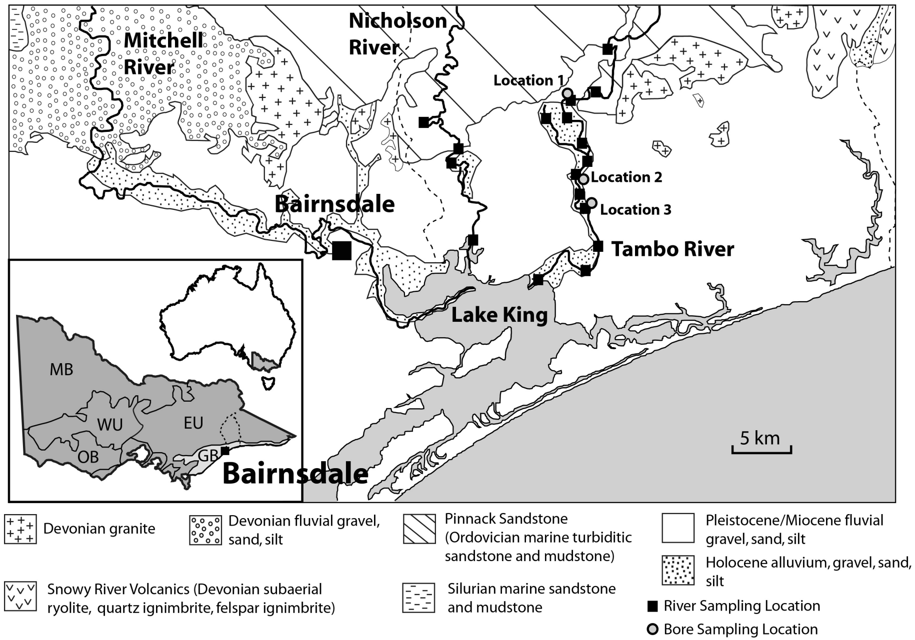

Fig. 1. Map of the Tambo River Basin (dashed line) with sampling locations on Tambo and Nicholson Rivers, and local surface geology (modified from Jolly 1997). GB = Gippsland Basin, EU = Eastern Victorian Uplands, WU = Western Victorian Uplands, OB = Otway Basin, MB = Murray Basin.

HESSD
10, 3795–3842, 2013
Groundwater – surface water interactions
N. P. Unland et al.

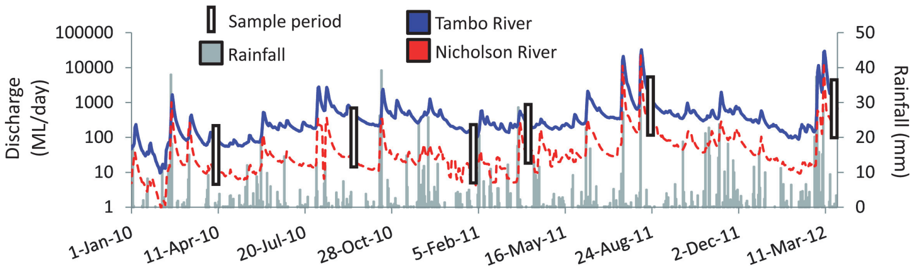

Fig. 2. Sampling frequency superimposed on river hydrographs (Tambo River = Battens Landing station 223 209, Nicholson River = Sarsfield gauging station 223 210) and rainfall in the Tambo Catchment (Bairnsdale Airport, station 85 279).

HESSD
10, 3795–3842, 2013

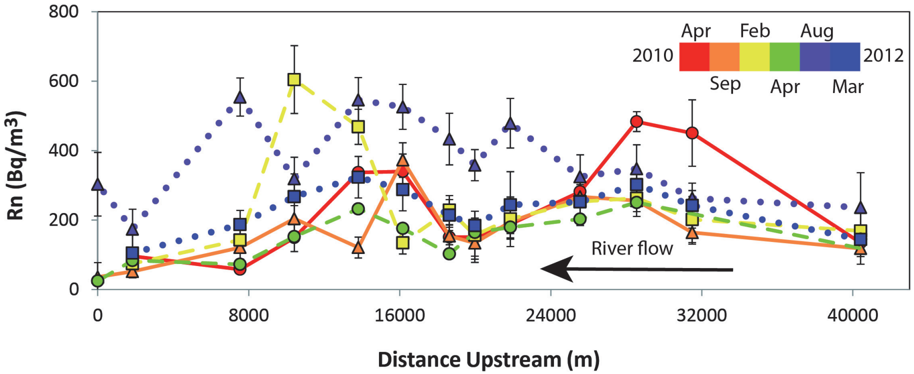

Fig. 3. Distribution of ^{222}Rn activities in water sampled from the Tambo River over the study period. April 2010 = solid line with circles, September 2010 = solid line with triangles, February 2011 = dashed line with squares, April 2011 = dashed lines with circles, August 2011 = dotted line with triangles, March 2012 = dotted line with squares.

HESSD
10, 3795–3842, 2013

Groundwater – surface water interactions

N. P. Unland et al.

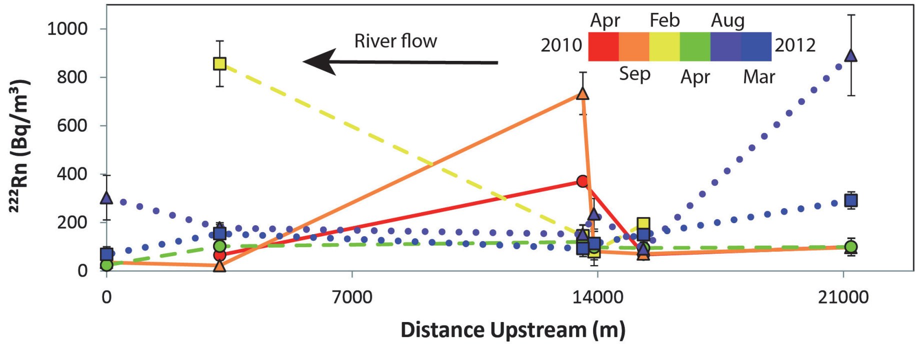

Fig. 4. Distribution of ^{222}Rn activities in water sampled from the Nicholson River over the study period. April 2010 = solid line with circles, September 2010 = solid line with triangles, February 2011 = dashed line with squares, April 2011 = dashed lines with circles, August 2011 = dotted line with triangles, March 2012 = dotted line with squares.

HESSD
10, 3795–3842, 2013

Groundwater – surface water interactions

N. P. Unland et al.

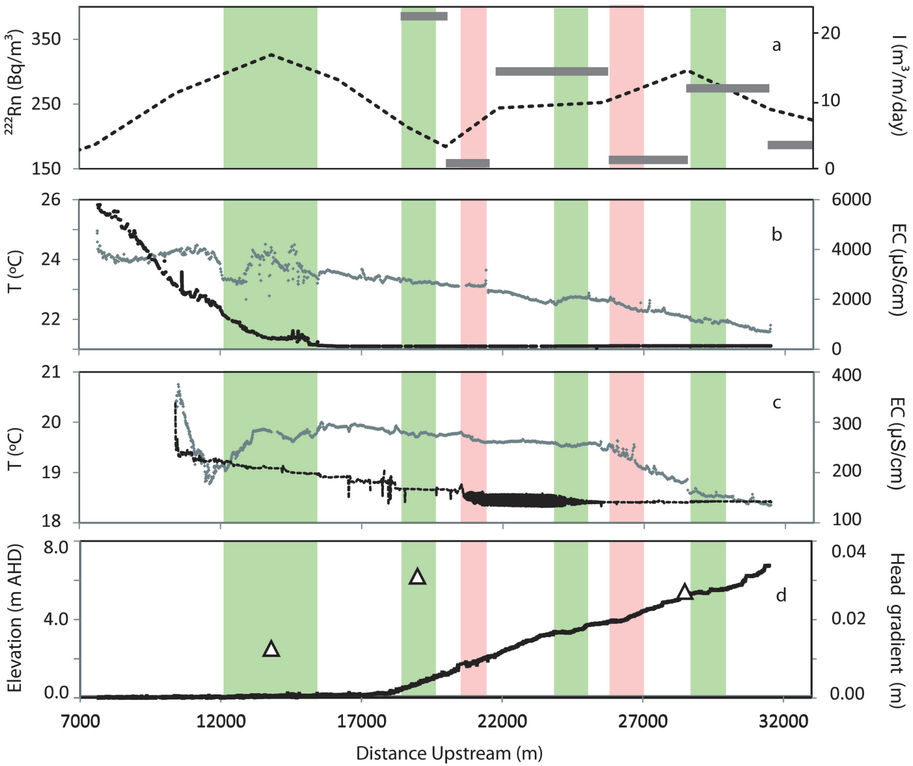

Fig. 5. Inferred zones of increased groundwater discharge (green shading) and decreased groundwater discharge (red shading) on the Tambo River as indicated by; **(a)** average ^{222}Rn activities (dashed line) and average groundwater fluxes by ^{222}Rn mass balance (grey bars), temperature (grey dots) and EC (black dots) profiles from Februaryruary 2011 **(b)** and Marchch 2012 **(c)**, average groundwater – surface water gradients (triangles) and surface water river elevation (black line) **(d)**.

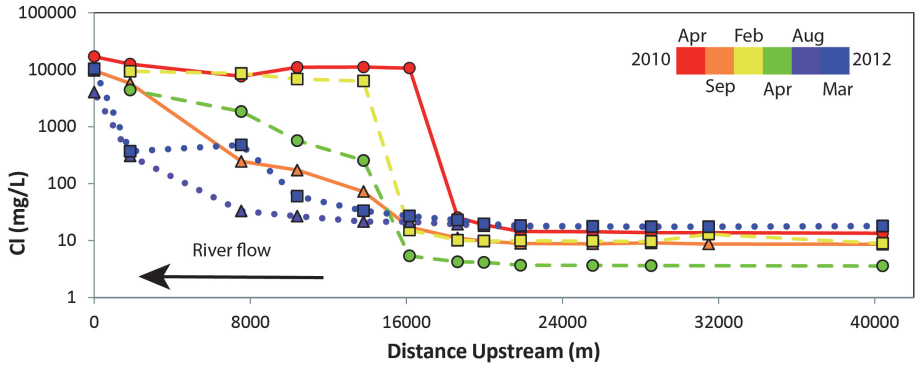

Fig. 6. Distribution of Cl concentrations in water sampled from the Tambo River over the study period. April 2010 = solid line with circles, September 2010 = solid line with triangles, February 2011 = dashed line with squares, April 2011 = dashed lines with circles, August 2011 = dotted line with triangles, March 2012 = dotted line with squares.

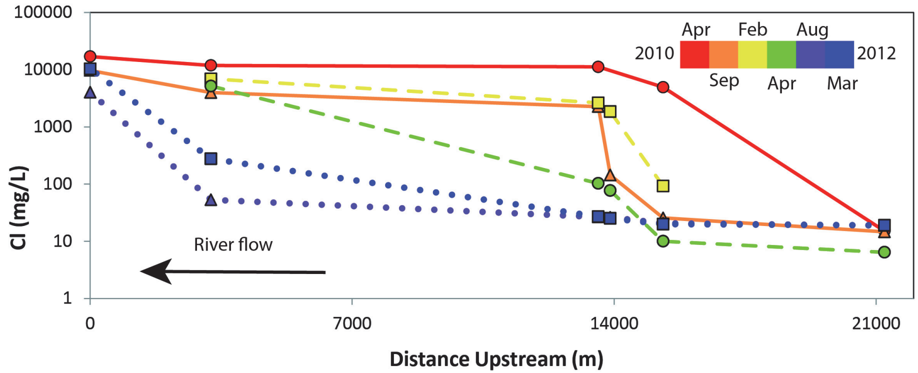

Fig. 7. Distribution of Cl concentrations in water sampled from the Nicholson River over the study period. April 2010 = solid line with circles, September 2010 = solid line with triangles, February 2011 = dashed line with squares, April 2011 = dashed lines with circles, August 2011 = dotted line with triangles, March 2012 = dotted line with squares.

HESSD
10, 3795–3842, 2013

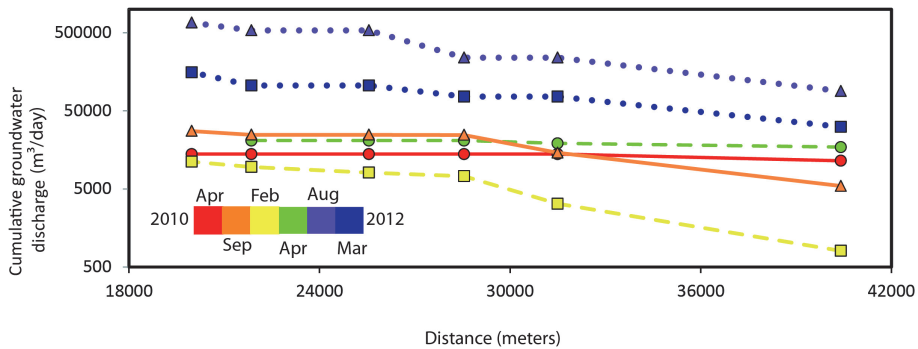

Fig. 8. Cumulative groundwater discharge to the Tambo River from ^{222}Rn mass balance. April 2010 = solid line with circles, September 2010 = solid line with triangles, February 2011 = dashed line with squares, April 2011 = dashed lines with circles, August 2011 = dotted line with triangles, March 2012 = dotted line with squares.

HESSD
10, 3795–3842, 2013

Groundwater – surface water interactions

N. P. Unland et al.

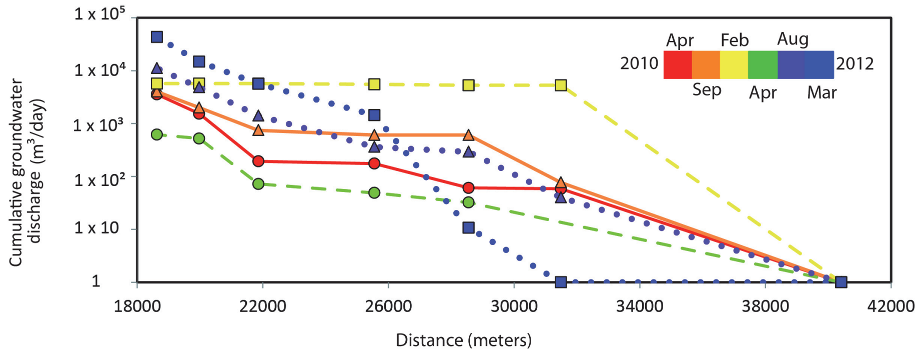

Fig. 9. Cumulative groundwater discharge to the Tambo River from Cl mass balance. April 2010 = solid line with circles, September 2010 = solid line with triangles, February 2011 = dashed line with squares, April 2011 = dashed lines with circles, August 2011 = dotted line with triangles, March 2012 = dotted line with squares.

HESSD
10, 3795–3842, 2013

Groundwater – surface water interactions

N. P. Unland et al.

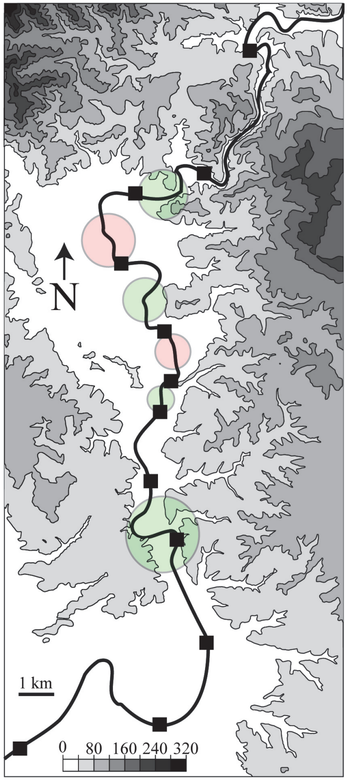

Fig. 10. Topographic map of the Tambo River with river sampling locations (black squares) and areas of increased (green shading) and decreased (red shading) groundwater discharge as indicated by Fig. 5.

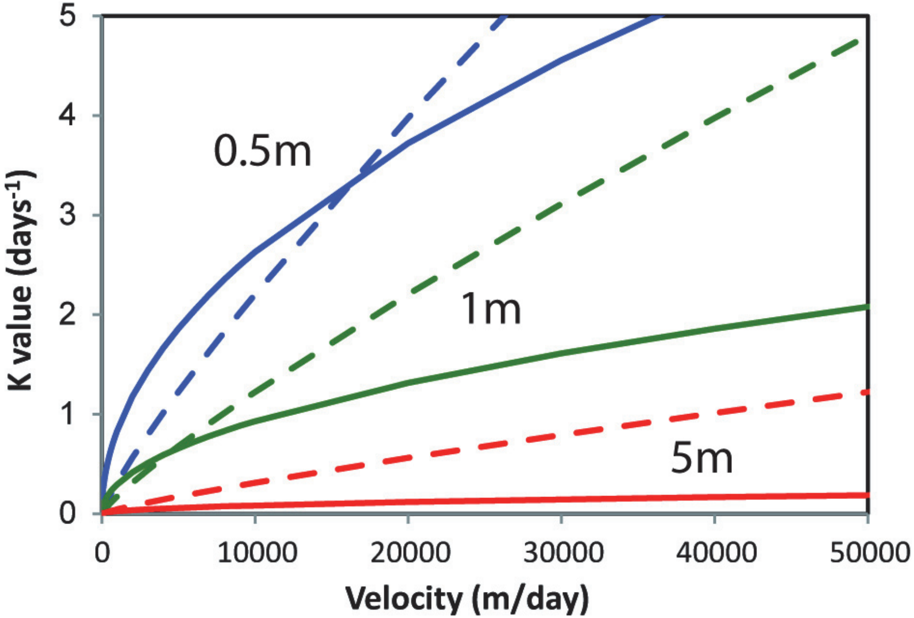

Fig. 11. *K* values from O'Connor and Dobins (solid lines) and Negulescu and Rohanski (dashed lines) models at 0.5 m (blue), 1 m (green) and 5 m depth (red) with increasing river velocities.

HESSD
10, 3795–3842, 2013

Groundwater – surface water interactions

N. P. Unland et al.

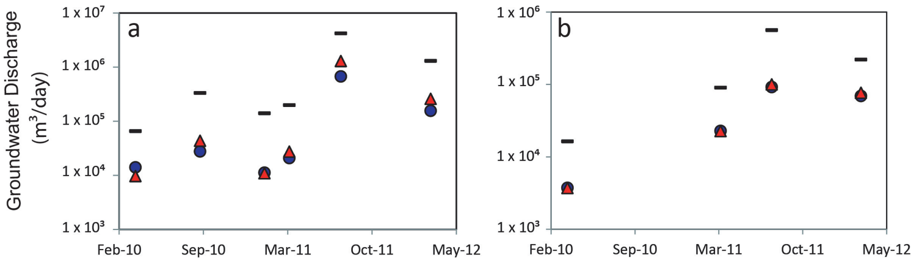

Fig. 12. Temporal variations in river discharge (black lines) and groundwater discharge to the Tambo River **(a)** and Nicholson River **(b)** given by ^{222}Rn mass balance using O'Connor and Dobins (blue circles) and Negulescu and Rojanski (red triangles) models of gas transfer.

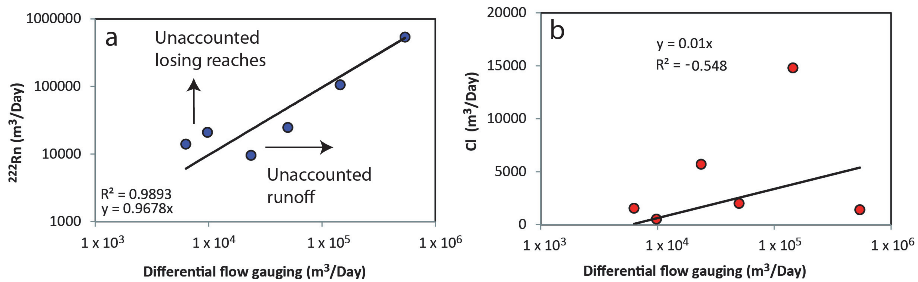

Fig. 13. Groundwater discharge to the Tambo River by differential flow gauging (x-axis) versus groundwater discharge given by ^{222}Rn mass balance **(a)** and Cl mass balance **(b)**.

HESSD
10, 3795–3842, 2013